Title

Accelerating Catalytic Oxyanion Reduction with Inert Metal Hydroxides

Journal

Environmental Science and Technology, 57(3)

ISSN

0013-936X

Authors

Gao, Jinyu
Zhao, Qiang
Tan, Cheng
et al.

Publication Date

2023-01-24

DOI

10.1021/acs.est.2c06468

Peer reviewed

Environmental Science & Technology

pubs.acs.org/est

Article

Accelerating Catalytic Oxyanion Reduction with Inert Metal Hydroxides

Jinyu Gao, Qiang Zhao, Cheng Tan, Shaohua Xie, Yadong Yin, Fudong Liu, Haizhou Liu, Baoliang Chen, and Jinyong Liu*

Cite This: *Environ. Sci. Technol.* 2023, 57, 1479−1486

Read Online

ACCESS | Metrics & More | Article Recommendations | Supporting Information

ABSTRACT: Adding Cr^{III} or Al^{III} salts into the water suspension of platinum group metal (PGM) catalysts accelerated oxyanion pollutant reduction by up to 600%. Our initial attempts of adding $K_2Cr^{VI}O_4$, $K_2Cr^{VI}_2O_7$, or $KCr^{III}(SO_4)_2$ into Pd/C enhanced BrO_3^- reduction with 1 atm H_2 by 6-fold. Instrument characterizations and kinetic explorations collectively confirmed the immobilization of reduced Cr^{VI} as $Cr^{III}(OH)_3$ on the catalyst surface. This process altered the ζ-potentials from negative to positive, thus substantially enhancing the Langmuir−Hinshelwood adsorption equilibrium constant for BrO_3^- onto Pd/C by 37-fold. Adding $Al^{III}(OH)_3$ from alum at pH 7 achieved similar enhancements. The Cr−Pd/C and Al−Pd/C showed top-tier efficiency of catalytic performance (normalized with Pd dosage) among all the reported Pd catalysts on conventional and nanostructured support materials. The strategy of adding inert metal hydroxides works for diverse PGMs (palladium and rhodium), substrates (BrO_3^- and ClO_3^-), and support materials (carbon, alumina, and silica). This work shows a simple, inexpensive, and effective example of enhancing catalyst activity and saving PGMs for environmental applications.

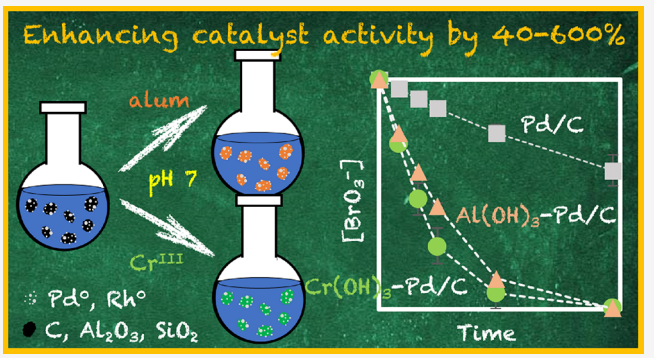

KEYWORDS: *aluminum, chromium, chlorate, bromate, catalyst support, zeta-potential, X-ray photoelectron spectroscopy (XPS), scanning transmission electron microscopy (STEM)*

INTRODUCTION

Heterogeneous catalysis has proven to be a clean and efficient approach to reducing toxic oxyanions (e.g., BrO_3^-, ClO_3^-, ClO_4^-, NO_3^-, and CrO_4^{2-}).[1−3] These oxyanions become water pollutants from both natural and engineered oxidative processes.[4−7] Platinum group metals (PGMs) such as Pd allow the use of 1 atm H_2 at ambient temperature for oxyanion reduction

$$BrO_3^- + 3H_2 \rightarrow Br^- + 3H_2O \quad (1)$$

$$ClO_3^- + 3H_2 \rightarrow Cl^- + 3H_2O \quad (2)$$

In particular, the catalysts have shown strong resistance to concentrated salts in various scenarios.[5,6,8] Hence, the catalytic reduction has a high promise to be integrated with separation (e.g., ion exchange) and other destruction technologies (e.g., electrochemical) for water and wastewater treatment.[8−10]

The high cost of PGMs has triggered numerous efforts to enhance the catalyst activity and thus reduce metal usage. One strategy is to increase the reaction rates on the catalyst surface. This can be achieved by either maximizing the PGM atom exposure[11,12] or incorporating a secondary metal to allow additional reaction mechanisms (e.g., Cu,[13] Sn,[14] and In[15] for NO_3^- reduction; Re[16−18] and Mo[6,7,10] for ClO_4^- reduction). The other strategy is to enhance substrate adsorption via surface modification. For example, nanostructured coatings provide extended surface area or tunable surface charge to improve mass transfer.[19,20] The catalyst support can be grafted or doped with nitrogen functional groups via various thermal procedures.[21−24] Doping metal oxides (e.g., CeO_2) via calcination could also enhance substrate adsorption.[25,26] Nevertheless, most reported strategies involve arduous materials synthesis or high-temperature treatment.

Previously, we have developed a highly active Mo−Pd/C catalyst family for ClO_3^- and ClO_4^- reduction.[6,7,10] The reduction of polymeric molybdates (from Na_2MoO_4) on the Pd/C surface yielded Mo oxides in +2 to +5 oxidation states. Reduced Mo sites enable rapid oxygen atom transfer (OAT) from the coordinated ClO_3^- and ClO_4^-. However, Na_2WO_4 did not enhance the reaction on the same Pd/C + H_2 platform. Curious about the trend among Group 6 elements (Cr, Mo,

Received: September 5, 2022
Revised: December 24, 2022
Accepted: December 27, 2022
Published: January 12, 2023

https://doi.org/10.1021/acs.est.2c06468
Environ. Sci. Technol. 2023, 57, 1479−1486

and W), we further examined the chemistry of K_2CrO_4 reduced on the Pd/C surface. Although the reduced Cr did not exhibit OAT activity as Mo, it surprisingly enhanced the activity of various supported Pd catalysts by 200−600% by forming $Cr(OH)_3$ on the catalyst surface. This report elucidates the underlying mechanism and applies the same approach to $Al(OH)_3$. This work showcases the saving of PGMs by significantly enhancing the catalyst activity in a simple but effective way.

MATERIALS AND METHODS

General Information. All chemicals and materials were purchased from Sigma-Aldrich or Alfa Aesar and used as received. Detailed information on support materials and commercial catalysts is described in Table S1 of the Supporting Information. Aqueous solutions were prepared with deionized (DI) water (resistivity >18.2 MΩ cm). Unless specified, all operations were conducted at room temperature (20 ± 1 °C). Pd/C, Pd/Al_2O_3, and Pd/SiO_2 catalysts were prepared by our recently developed all *in situ* method.[5] To prepare a batch of Pd catalyst for multiple uses, a 500 mL round bottom flask was sequentially loaded with a magnetic stir bar, 40 mg of support (C, Al_2O_3, or SiO_2), DI water (400 mL), and the desired amount of Na_2PdCl_4 (dissolved in a stock solution). The flask was capped with a rubber stopper and sonicated for 1 min. The suspension was then stirred at 350 rpm for 5 min to allow Pd^{II} adsorption onto the support. After that, H_2 gas (99.999% by Airgas, about 10 mL min^{-1}) was supplied through a 16-gauge stainless steel needle penetrating the stopper. The second needle served as both the gas outlet and sampling port. Another 5 min was allowed to reduce adsorbed Pd^{II} and yield supported Pd^0 catalysts. The solid catalyst was collected on filter paper and dried by airflow in a fume hood. This method has been fully validated in our previous study.[5] A 4 mg portion of the catalyst powder was used for the next step. For a one-pot preparation for single use, a 200 mL round bottom flask was sequentially loaded with a magnetic stir bar, 4 mg of support, DI water (200 mL), and Na_2PdCl_4. All the following procedures (without filtration) are the same as described above. The prepared catalyst suspension was ready for Cr or Al addition.

Preparation of Cr- and Al-Enhanced Catalysts. For the typical Cr−Pd/C, a magnetic stir bar, 4 mg of Pd/C, 200 mL of DI water, and the desired amount of the Cr precursor (dissolved in a stock solution) were added in a 200 mL round bottom flask. The initial pH was adjusted to 3.0 by 0.1 N H_2SO_4 to supply the H^+ consumption for Cr^{VI} reduction (from the K_2CrO_4 or $K_2Cr_2O_7$ precursor)

$$Cr_2O_7^{2-} + 8H^+ + 3H_2 \rightarrow 2Cr^{3+} + 7H_2O \quad (3)$$

$$2CrO_4^{2-} + 10H^+ + 3H_2 \rightarrow 2Cr^{3+} + 8H_2O \quad (4)$$

The mixture was sonicated for 1 min and then sparged with H_2 (about 2 mL min^{-1}) under stirring for 1 h (not optimized) to allow the complete reduction of Cr^{VI} and any surface oxide on Pd nanoparticles. For the Cr^{III} precursor, $KCr(SO_4)_2$, and the Al^{III} precursor, $KAl(SO_4)_2$, 10 min of H_2 sparging was used. Then, the pH was adjusted to 7.0 by 0.1 N NaOH to trigger the formation of $Cr(OH)_3$ or $Al(OH)_3$. The operation with other Pd or Rh catalysts on Al_2O_3 or SiO_2 followed the same procedure. The concentration of total Cr in aqueous samples was monitored by inductively coupled plasma-mass spectrometry (ICP−MS, Agilent 7700).

Catalytic BrO_3^- and ClO_3^- Reduction. At pH 7.0, $KBrO_3$ (dissolved in a stock solution) was added at designated concentrations to the water suspension of Pd catalysts (0.02 g L^{-1}), and $NaClO_3$ was added to the water suspension of Rh catalysts (0.5 g L^{-1}). The H_2 flow was maintained at about 2 mL min^{-1}. Aqueous samples were collected with a 3 mL syringe and immediately filtered through a 0.22 μm cellulose acetate membrane. Anions (BrO_3^-, Br^-, ClO_3^-, and Cl^-) were determined by ion chromatography (Dionex ICS−5000) with a conductivity detector, a 25 μL injection loop, an IonPac AS19 column at 30 °C, and 20 mM KOH eluent at 1 mL min^{-1}.

Catalytic Characterization. The freshly prepared Cr−Pd/C suspension was immediately transferred into an anaerobic glove bag (98% N_2, 2% H_2; Coy Laboratories) to avoid artifacts from air oxidation. The suspension was vacuum-filtered, and the filter cake was placed in a 20 mL scintillation vial and dried in a 110 °C sand bath for 8 h. The catalyst powder was loaded onto a copper conductive tape and transported inside an anaerobic tube to the XPS instrument (AXIS Supra Kratos Analytical, equipped with a monochromatized Al Kα source). The sp^2 C 1s peak (285.0 eV) of the carbon support was used for binding energy (BE) calibration. The Cr 2p and Pd 3d spectra were fitted by constraining the separation of characteristic doublet peaks (9.50 eV for Cr and 5.27 eV for Pd) and the ratio of doublet peak areas (2:1 for Cr and 3:2 for Pd) using CasaXPS software (version 2.3.19). For the characterization by scanning transmission electron microscopy (STEM, FEI Titan Themis 300, with an energy-dispersive X-ray spectrometer (EDS) at 300 kV accelerating voltage), the dried catalyst was redispersed in distilled water and sonicated for 30 min. A drop of the suspension was loaded onto the copper microgrids and dried under vacuum. The STEM images were acquired with a high-angle annular dark-field (HAADF) detector. The zeta-potentials of the catalysts were measured using a zeta-potential and submicron particle size analyzer (DelsaNano C, Beckman Coulter). The specific surface areas of Pd in Pd/C and Cr−Pd/C were determined by CO pulse titration (Pd:CO stoichiometry at 2:1) on a Quantachrome Autosorb-iQ physisorption−chemisorption instrument.

RESULTS AND DISCUSSION

Significantly Accelerated BrO_3^- Reduction by Cr. Adding either the Cr^{III} or Cr^{VI} precursor into Pd/C substantially accelerated BrO_3^- reduction (Figure 1a). At pH 7 and 20 °C, the Cr−Pd/C catalyst at 0.02 g L^{-1} achieved >99% reduction of 1 mM BrO_3^- within 1 h. The good Br balance between BrO_3^- and Br^- throughout the reaction (Figure S1) indicates the complete reduction with no accumulation of other Br intermediates. Under the same reaction settings, Pd/C (without Cr addition) reduced only 40% of the initial BrO_3^-. In our previous report,[5] a five-fold loading (0.1 g L^{-1}) of Pd/C reduced 95% of the initial BrO_3^-. Apparently, the addition of Cr could save >80% of Pd while ensuring the same catalytic performance. We summarized various Pd catalysts for BrO_3^- reduction[4,5,20,25,27−33] in Table S2. Direct comparison among different reports is challenging because the catalysts were tested under different pH and temperatures. The increase in pH significantly decreased the reaction rate. Even the reaction rate at 25 °C could be twice the rate at 20 °C.[30] For a coarse evaluation, we normalized the initial zeroth-order rate of BrO_3^- reduction (mmol L^{-1} min^{-1})

https://doi.org/10.1021/acs.est.2c06468
Environ. Sci. Technol. 2023, 57, 1479−1486

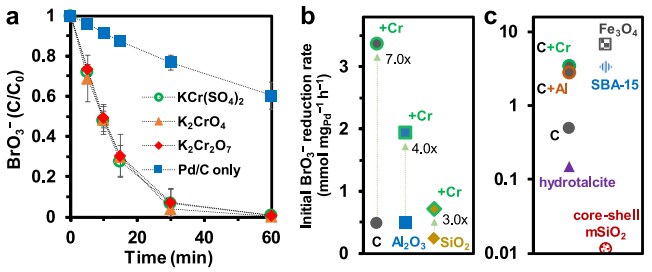

Figure 1. (a) Time profiles of BrO_3^- reduction by Pd/C added with various Cr precursors (5 wt % as Cr). Reaction conditions: 0.02 g L^{-1} 5 wt % Pd/C, 1 mM BrO_3^-, pH 7, 1 atm H_2, and 20 °C; (b) initial rate of 1 mM BrO_3^- reduction by Pd catalysts prepared using various kinds of support before and after Cr addition; and (c) rate comparison of Cr- and Al-added Pd/C with various supported Pd catalysts tested at pH 6.9−8.0 (see Table S2). The rates have been normalized by the Pd dosage.

by the amount of Pd in the system (mg$_{Pd}$ L^{-1}). Cr−Pd/C showed a 6-fold higher initial BrO_3^- reduction rate than Pd/C (Figure 1b) and is among the top performers in the pH range of 6.9−8.0 (Figure 1c). The only reported catalyst that showed a higher activity used nanostructured iron oxide support, and the reaction was conducted at 27 °C.[31] More importantly, the preparation of Cr−Pd/C does not involve nanostructuring of the support material.

Characterization of Surface Cr Species. At first, we assumed that Cr^{VI} could follow a similar redox mechanism as Mo^{VI}, which is underneath Cr in the periodic table. In the Mo−Pd/C system, the Mo^{VI} precursor is reduced by H_2 + Pd/C into multiple low-valent Mo species that remove the oxygen atoms stepwise from coordinated ClO_x^- substrates.[6] However, XPS characterization of the Cr−Pd/C prepared from Cr^{VI} precursors only found one single Cr 2p$_{3/2}$ peak (BE of 577.2 eV from $Cr_2O_7^{2-}$ and 577.7 eV from CrO_4^{2-}; Figure 2a). The

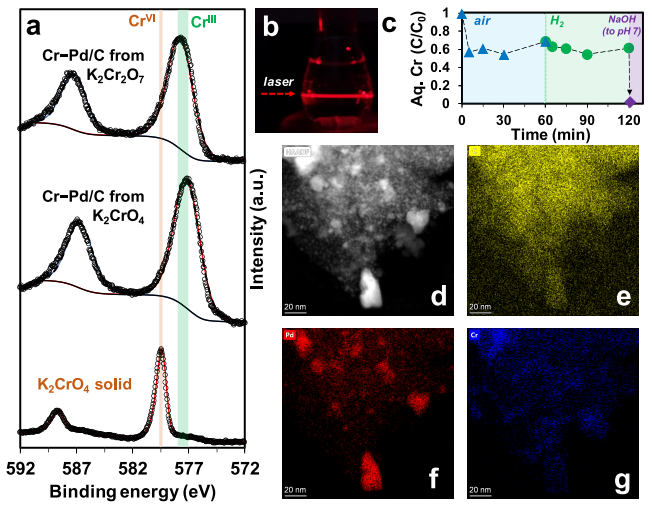

Figure 2. (a) Cr 2p XPS spectra of the Cr^{VI} reference (K_2CrO_4) and the 5 wt % Cr−5 wt % Pd/C prepared from K_2CrO_4 and $K_2Cr_2O_7$. The Cr 2p peaks in the K_2CrO_4 sample had minor tails originating from charge-up;[37] (b) Tyndall effect by colloids in aqueous $KCr(SO_4)_2$ solution (1 mg L^{-1} as Cr) at pH 7; (c) aqueous Cr concentration after adding $KCr(SO_4)_2$ (1 mg L^{-1} as Cr) into the Pd/C suspension and changing conditions; (d) HAADF-STEM imaging and EDS mapping of (e) C, (f) Pd, and (g) Cr of Cr−Pd/C prepared from $KCr(SO_4)_2$.

BE values closely match those for $Cr^{III}(OH)_3$ in the literature (576.7−577.6 eV).[34] The formation of $Cr^{III}{}_2O_3$ can be excluded because its Cr 2p$_{3/2}$ signal is a multiple-peak envelope typically fitted with five multiplet splitting peaks.[34,35] The exclusive formation of $Cr(OH)_3$ is consistent with the literature report on Pd-catalyzed reduction of Cr^{VI} oxyanions.[36] Hence, H_2 + Pd/C cannot reduce Cr^{III} further to lower oxidation states. The control experiment between 0.01 mM BrO_3^- and 0.1 mM $Cr(OH)_3$ (with H_2 but without Pd/C) found no reaction (Figure S2), thus excluding the Cr^{III}-mediated oxygen atom transfer mechanism.

Because all three Cr precursors yielded the same BrO_3^- reduction activity (Figure 1a), we continued the investigation with $KCr^{III}(SO_4)_2$. The dissolution of Cr^{3+} lowered the solution pH from 6.5 to 4.7, indicating the deprotonation of aqua complexes[38,39]

$$[Cr(H_2O)_x(OH)_{6-x}]^{(x-3)+} \rightarrow [Cr(H_2O)_{x-y}(OH)_{6-x+y}]^{(x-y-3)+} + yH^+ \quad (0 \le y \le x \le 6) \quad (5)$$

The addition of NaOH (to pH 7) generated Cr^{III} colloids (Figure 2b), suggesting the formation of $Cr(OH)_3{\cdot}3H_2O$ as a polymer[38−41]

$$[Cr(H_2O)_{x-y}(OH)_{6-x+y}]^{(x-y-3)+} + (x-y-3)\,OH^- \rightarrow Cr(OH)_3{\cdot}3H_2O + (x-y-3)\,H_2O \quad (6)$$

ICP−MS analysis of the filtered aqueous sample found that 43% of the initially added Cr^{III} (1 mg L^{-1} as Cr) was adsorbed onto Pd/C within 5 min. Whether or not applying H_2 did not impact Cr adsorption (Figure 2c). The subsequent NaOH addition to pH 7 led to >98% of Cr removal from the aqueous phase. Elemental analysis of the resulting solid found 3.5 wt % of Cr and 4.3 wt % of Pd, both of which were close to a theoretical value of 4.4 wt % (i.e., 5 mg of Cr as $Cr(OH)_3$ and 5 mg of Pd^0 added to 100 mg of carbon). We note that not all Cr are necessarily in the Pd/C because some $Cr(OH)_3$ might have precipitated as a bulk solid together with Pd/C. However, STEM−EDS characterization on individual Cr−Pd/C catalyst particles observed Cr throughout the surface, either on the carbon support or overlapping with Pd particles (Figure 2d−g). The exclusive metallic state of Pd was confirmed by the XPS Pd 3d$_{5/2}$ BE at 335.80 eV (Figure S3).

Effect of Surface Cr Species. For the 5 wt % Pd/C catalyst, the activity showed an apparent increase upon adding the nominal Cr content to 5 wt % (Table 1, entries 1−3). Further increasing the Cr content above 5 wt % resulted in lower reaction rates (Table 1, entries 3−5). This was probably due to the partial coverage of the Pd surface by $Cr(OH)_3$. For the 1 wt % Pd/C catalyst, apparent activity improvement was observed upon adding 1 wt % Cr. Increasing the Cr content to 2.5 wt % and above also resulted in lower reaction rates (Table 1, entries 6−9). For the 0.5 wt % Pd/C catalyst, Cr addition adversely lowered the activity (Table 1, entries 10−13). In our previous study,[5] we observed that the average size of Pd^0 particles (>90% in 1−6 nm, 37% in 2−3 nm) in 5 wt % Pd/C was twice that in 0.5 wt % Pd/C (>90% in 0.5−2 nm, 48% in 1−1.5 nm). It appears that the surface $Cr(OH)_3$ could inhibit the interaction between BrO_3^- and Pd, particularly for <2 nm Pd^0 particles. Notably, CO chemisorption did not observe a significantly altered Pd dispersion value upon Cr addition

https://doi.org/10.1021/acs.est.2c06468
Environ. Sci. Technol. 2023, 57, 1479−1486

Table 1. Zeroth-Order Rate Constants of BrO_3^- Reduction by Cr−Pd/C and Pd/C with Various Metal Contents

entry	Pd wt%[a]	Cr wt%[a]	k(mmol g_{cat}^{-1} min^{-1})
1	5	0	0.39 ± 0.07[b]
2	5	2.5	1.98 ± 0.23
3	5	5	2.42 ± 0.27
4	5	7.5	2.18 ± 0.40
5	5	10	1.71 ± 0.20
6	1	0	0.27 ± 0.04[b]
7	1	1	0.42 ± 0.03
8	1	2.5	0.36 ± 0.04
9	1	5	0.28 ± 0.01
10	0.5	0	0.19 ± 0.03[b]
11	0.5	1	0.18 ± 0.02
12	0.5	2.5	0.14 ± 0.02
13	0.5	5	0.08 ± 0.01

[a]Nominal values based on the amounts of metal added. As evidenced by ICP−MS analysis, both Pd and Cr were absent in the aqueous phase. However, not all $Cr(OH)_3$ is necessarily dispersed on the carbon support. Aggregation of bulk $Cr(OH)_3$ particles is possible. [b]The BrO_3^- reduction using Pd/C without Cr addition followed first-order kinetics. For direct comparison with Cr−Pd/C that showed zeroth-order kinetics in the beginning, we fit the BrO_3^- concentration decrease in the initial 5 min with the zeroth-order model.

(16.1% for the 5 wt % Pd/C versus 15.7% after 5 wt % Cr was added). The CO mass transfer at the gas−solid interface does not necessarily reflect the behavior of hydrated anions at the water−solid interface. In addition, chemisorption experiments involved heating processes that might alter the morphology of Pd and Cr species formed *in situ* at 20 °C. Therefore, a quantitative description of Pd coverage was not established. However, the more important information is that the most effective activity enhancement is for catalysts with relatively large metal particles (e.g., >2 nm).

While the activity of Pd/C increased with the decreasing pH (Figure 3a),[4,28,31] the activity of Cr−Pd/C at pH 5 was slightly lower than at pH 7 (Figure 3b). Visual MINTEQ simulation suggested that $Cr(OH)_3$ started dissolution at pH <6 (Figure 3c). At pH 7, the stability of $Cr(OH)_3$ on the Pd/C was demonstrated by several observations. First, the collection of the Cr−Pd/C solid by filtration and the redispersion in water by sonication resumed the high activity (Figure S4), showing that the Cr on Pd/C could resist a common mechanical disturbance. Second, the Cr in the aqueous phase during BrO_3^- reduction was below 2% of the total Cr added (Figure S5). Third, the catalyst maintained the same high activity for five continuous BrO_3^- spikes (Figure S6), indicating no significant loss of immobilized Cr upon extended use.

Role of Surface Cr. Because the chemical reaction between BrO_3^- and $Cr(OH)_3$ has been ruled out, we further examined the role of $Cr(OH)_3$ in the modification of the catalyst surface, which is critical for substrate adsorption.[20] At pH 7, the addition of Cr reversed the ζ-potential of Pd/C from negative to positive (Table 2, entry 1). It appears that the positively charged surface enhanced BrO_3^- adsorption to the catalyst via electrostatic interaction. The fresh $Cr(OH)_3$ colloids prepared

Table 2. Zeta-Potentials of Different Catalysts at pH 7

entry	catalyst	ζ-potential without Cr (mV)	ζ-potential with Cr (mV)
1	Pd/C	−52.4 ± 8.9	30.2 ± 1.4 (26.7 ± 2.6 with Al)
2	Pd/Al_2O_3	0.55 ± 0.57	24.9 ± 2.6
3	Pd/SiO_2	−14.5 ± 2.8	21.6 ± 1.8
4	Rh/C	−55.8 ± 7.6	5.7 ± 1.7

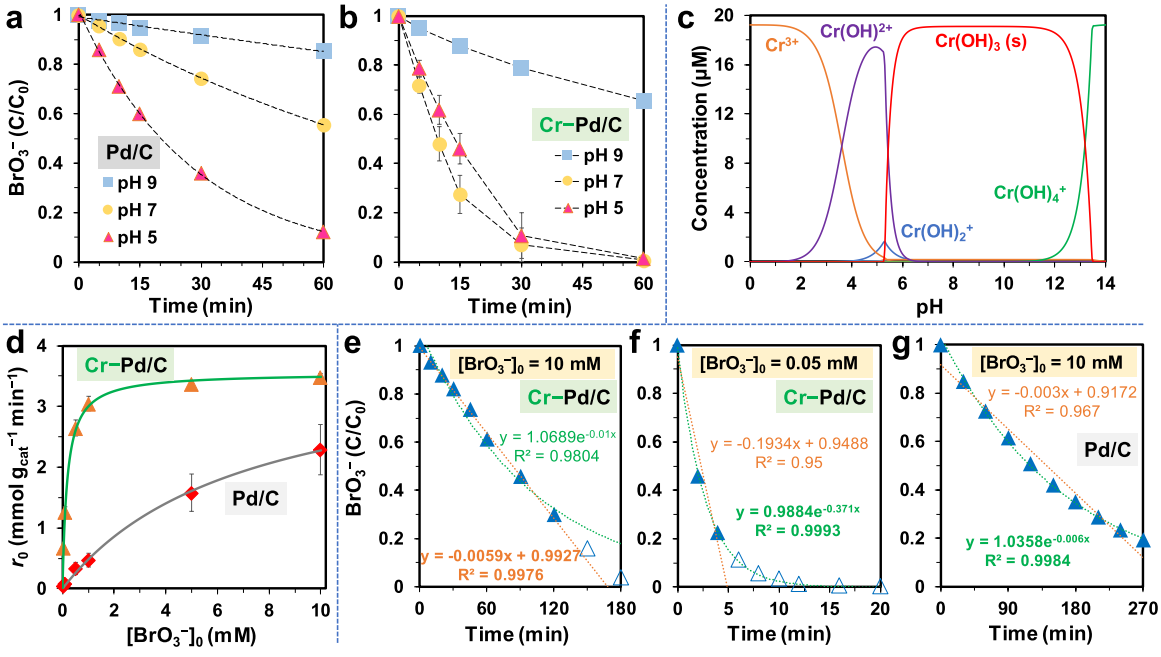

Figure 3. Time profiles of 1 mM BrO_3^- reduction by (a) Pd/C and (b) Cr−Pd/C; (c) calculated Cr^{III} speciation in the aqueous solution (1 mg L^{-1} as Cr, Visual MINTEQ ver. 3.1); (d) initial rate of BrO_3^- reduction at various initial BrO_3^- concentrations and the LH model fits; (e−g) time profiles and modeling fitting results using the zeroth-order (linear) and first-order (exponential) kinetics. Reaction conditions: 0.02 g L^{-1} catalyst (5 wt % for each metal), 1 atm H_2, and 20 °C.

https://doi.org/10.1021/acs.est.2c06468
Environ. Sci. Technol. 2023, 57, 1479−1486

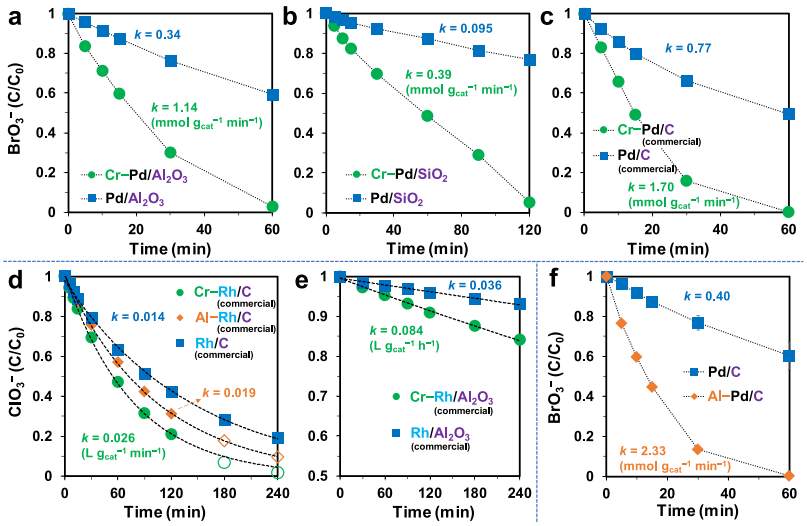

Figure 4. Reduction of 1 mM BrO_3^- using 0.02 g L^{-1} (a) Pd/Al_2O_3, (b) Pd/SiO_2, and (c) commercial Pd/C; reduction of 1 mM ClO_3^- using 0.5 g L^{-1} (d) Rh/C and (e) Rh/Al_2O_3 with and without Cr addition. The results upon Al addition to Rh/C and Pd/C are shown in panels (d) and (f), respectively. Reaction conditions: 5 wt % for each metal, pH 7, 1 atm H_2, and 20 °C.

by adjusting the aqueous solution of $KCr(SO_4)_2$ to pH 7 (Figure 2b) showed a similar ζ-potential of 34.0 ± 3.6 mV. However, the same Cr addition procedure applied to other catalysts resulted in different ζ-potentials (Table 2, entries 2–4). Thus, the measured ζ-potentials reflect the surface charge of the Cr-added catalysts rather than suspended $Cr(OH)_3$ solids that are not associated with catalyst particles.

The essential role of the surface Cr is further confirmed by kinetic analysis with the Langmuir–Hinshelwood (LH) model. Since the internal and external mass transfer limitations are both negligible (Text S1), the LH kinetic model is expressed as

$$r = \frac{K_1 k_3 [A]}{K_1 [A] + 1} \tag{7}$$

where r is the apparent rate of BrO_3^- reduction (mmol g_{cat}^{-1} min^{-1}), K_1 is the adsorption equilibrium constant (L $mmol^{-1}$) for BrO_3^-, k_3 is the rate constant (mmol g_{cat}^{-1} min^{-1}) for BrO_3^- reduction on the catalyst surface, and $[A]$ is the BrO_3^- concentration in the bulk aqueous phase (mmol L^{-1}). Text S2 provides the detailed derivation for eq 7.

The initial rates of BrO_3^- reduction r at various initial BrO_3^- concentrations at pH 7 were fit to eq 7 (Figure 3d). The corresponding adsorption equilibrium constant K_1 for Cr–Pd/C (5.44 L $mmol^{-1}$) was more than 37-fold larger than that for Pd/C (0.14 L $mmol^{-1}$), confirming that the positively charged $Cr(OH)_3$ on the catalyst surface enhanced BrO_3^- adsorption. On the other hand, the rate constant k_3 for Cr–Pd/C (3.55 mmol g_{cat}^{-1} min^{-1}) is slightly smaller than that for Pd/C (3.88 mmol g_{cat}^{-1} min^{-1}). This is consistent with the early postulation that a small portion of the Pd^0 particle surface is covered by $Cr(OH)_3$, resulting in a reduced number of active sites compared to the bare Pd/C.

The kinetic pattern with Cr–Pd/C was first order at low $[BrO_3^-]_0$ and zeroth order at high $[BrO_3^-]_0$ (Figure S7). This switch can be readily explained by the LH model. At high BrO_3^- concentrations (e.g., 1, 5, and 10 mM), $K_1[A] \gg 1$ so that eq 7 can be simplified to the zeroth-order expression (Figure 3e)

$$r = k_3 \tag{8}$$

At low BrO_3^- concentrations (e.g., 0.05 and 0.1 mM), $K_1[A] \ll 1$ so that eq 7 evolves to the first-order expression (Figure 3f)

$$r = K_1 k_3 [A] \tag{9}$$

In stark contrast, the bare Pd/C catalyst showed the first-order kinetics for all $[BrO_3^-]_0$ at 0.05–10 mM (Figure 3g and Figure S8 for all conditions) because the small K_1 (0.14 L $mmol^{-1}$) could only allow the expression of eq 9.

Extension to Other Catalysts and $Al(OH)_3$ Addition. From the same protocols for supported Pd^0 catalyst preparation and $Cr(OH)_3$ addition, the immobilized Cr also enhanced the BrO_3^- reduction activity of 5 wt % Pd/Al_2O_3 and 5 wt % Pd/SiO_2 by 235 and 310%, respectively (Figure 4a,b, data fit with the zeroth-order model). These results are consistent with the alteration of ζ-potentials (Table 2). We also confirmed the adaptability of this strategy to a commercial 5 wt % Pd/C catalyst (Figure 4c). Besides BrO_3^- reduction, we further examined the same strategy to enhance the reduction of ClO_3^-, a much more recalcitrant oxyanion pollutant for Pd catalysts. We used a different metal, Rh, which is superior to Pd for ClO_3^- reduction at pH 7.[4] As expected, the $Cr(OH)_3$ addition increased the first-order rate constants of the commercial 5 wt % Rh/C and 5 wt % Rh/Al_2O_3 by 86 and 133%, respectively (Figure 4d,e).

As Cr^{III} is potentially toxic,[42] we further explored the possibility of using other trivalent metal hydroxides that can play a similar role as $Cr(OH)_3$. At the circumneutral pH, Al^{3+} precipitates into $Al(OH)_3$, an amphoteric compound analogous to $Cr(OH)_3$. In addition, it is not readily reducible by H_2 like $Fe(OH)_3$.[43] As the common coagulant for drinking water treatment, $Al(OH)_3$ does not trigger particular concerns about toxicity or cost. Following the same protocol for $Cr(OH)_3$–Pd/C, we prepared the $Al(OH)_3$–Pd/C. Elemental analysis found 4.9 wt % of Al and 4.3 wt % of Pd, which are both close to a theoretical value of 4.2 wt % (i.e., 5 mg of Al as $Al(OH)_3$ and 5 mg of Pd^0 added to 100 mg of carbon). BrO_3^- reduction kinetics showed that $Al(OH)_3$ increased the zeroth-order rate constant by 480% (Figure 4f). $Al(OH)_3$ also changed the ζ-potential of Pd/C to positive (Table 2, entry 1). The addition

https://doi.org/10.1021/acs.est.2c06468
Environ. Sci. Technol. 2023, 57, 1479–1486

of $Al(OH)_3$ to the commercial 5 wt % Rh/C also accelerated ClO_3^- reduction by 39% (Figure 4d).

Implications to Water Pollutant Degradation Technologies. The results in this study show that $Cr(OH)_3$, $Al(OH)_3$, and potentially other inert metal hydroxides on various PGM catalysts can modify the surface charge, boost the kinetics, and eventually save precious PGMs for water treatment applications. Multiple examples show that the simple immobilization of common hydrolyzable metal ions, such as Cr^{3+} and Al^{3+}, can achieve effective surface property tuning and substantially enhance the catalyst activity. More importantly, no expensive materials or complex procedures are involved in the catalyst preparation (Figure 1c). This feature is highly desirable for environmental applications. One immediate scenario is the potential acceleration of oxyanion reduction in the presence of the widespread Cr^{VI} co-contaminants (Figure 1a). Another scenario is the use of existing PGM catalysts with higher efficiency. Although we have found that 1 or 0.5 wt % Pd/C showed much higher cost-effectiveness than 5 wt % Pd/C,[5,10] many commercial catalysts contained 5 wt % PGM. If the users already obtained those high-metal content catalysts, then a simple treatment with alum addition at pH 7 is expected to substantially enhance the catalyst activity for anionic pollutant degradation.

In previously reported bimetallic catalysts, the secondary metals were primarily introduced as the novel reactive sites.[6,13−16] This work demonstrates a different aspect by integrating inert metal species to enhance mass transfer. While multiple data sets have confirmed both the presence (e.g., STEM−EDS characterization) and the critical role (pollutant degradation kinetics and LH modeling) of the metal hydroxides on the catalyst surface, some metal hydroxides might form independent aggregates outside the catalyst particles. The use of non-harmful metal hydroxides could minimize concerns about metal dissolution during engineering applications. The total solubility of various Al ions from $Al(OH)_3$ is 30−100 $\mu g\ L^{-1}$ at pH 7−8,[44] while the total solubility of Cr from $Cr(OH)_3$ is <50 $\mu g\ L^{-1}$ at pH 6−11.[45] Further evaluation of the catalyst robustness (i.e., activity and longevity under various conditions) is warranted. However, rather than including a very limited number of "representative" water matrix components herein, we recommend (i) serious and comprehensive testing under various real or simulated harsh conditions and (ii) developing technical solutions to the identified challenges, upon the selection of a specific practical application scenario.[10] It is also worth exploring the extension of this catalyst improvement strategy to other anionic pollutants (e.g., halogenated organic acids) and other catalytic mechanisms (e.g., advanced oxidation).

■ ASSOCIATED CONTENT

Supporting Information

The Supporting Information is available free of charge at https://pubs.acs.org/doi/10.1021/acs.est.2c06468.

Detailed information on support materials and commercial catalysts; literature summary of Pd catalysts for bromate reduction; additional kinetic and characterization data; discussion of reaction kinetics fitting and mass transfer limitation (PDF)

■ AUTHOR INFORMATION

Corresponding Author

Jinyong Liu − *Department of Chemical and Environmental Engineering, University of California, Riverside, California 92521, United States;* orcid.org/0000-0003-1473-5377; Email: jinyongl@ucr.edu, jinyong.liu101@gmail.com

Authors

Jinyu Gao − *Department of Chemical and Environmental Engineering, University of California, Riverside, California 92521, United States;* orcid.org/0000-0002-1751-3430

Qiang Zhao − *Department of Environmental Science, Zhejiang University, Hangzhou, Zhejiang 310058, China*

Cheng Tan − *Department of Chemical and Environmental Engineering, University of California, Riverside, California 92521, United States;* orcid.org/0000-0001-5878-6542

Shaohua Xie − *Department of Civil, Environmental, and Construction Engineering, Catalysis Cluster for Renewable Energy and Chemical Transformations (REACT), NanoScience Technology Center (NSTC), University of Central Florida, Orlando, Florida 32816, United States;* orcid.org/0000-0003-1550-7421

Yadong Yin − *Department of Chemistry, University of California, Riverside, California 92521, United States;* orcid.org/0000-0003-0218-3042

Fudong Liu − *Department of Civil, Environmental, and Construction Engineering, Catalysis Cluster for Renewable Energy and Chemical Transformations (REACT), NanoScience Technology Center (NSTC), University of Central Florida, Orlando, Florida 32816, United States;* orcid.org/0000-0001-8771-5938

Haizhou Liu − *Department of Chemical and Environmental Engineering, University of California, Riverside, California 92521, United States;* orcid.org/0000-0003-4194-2566

Baoliang Chen − *Department of Environmental Science, Zhejiang University, Hangzhou, Zhejiang 310058, China;* orcid.org/0000-0001-8196-081X

Complete contact information is available at: https://pubs.acs.org/10.1021/acs.est.2c06468

Notes

The authors declare no competing financial interest.

■ ACKNOWLEDGMENTS

Financial support was provided by the National Science Foundation (NSF CBET-1932942 for J.G. and J.L.). Dr. Krassimir Bozhilov performed the STEM characterization at the Central Facility for Advanced Microscopy and Microanalysis at UC Riverside. Dr. Ich Tran assisted in the XPS characterization performed at the UC Irvine Materials Research Institute using instrumentation funded in part by the NSF Major Research Instrumentation Program (CHE-1338173).

■ REFERENCES

(1) Chaplin, B. P.; Reinhard, M.; Schneider, W. F.; Schüth, C.; Shapley, J. R.; Strathmann, T. J.; Werth, C. J. Critical review of Pd-based catalytic treatment of priority contaminants in water. *Environ. Sci. Technol.* **2012**, *46*, 3655−3670.

(2) Yin, Y. B.; Guo, S.; Heck, K. N.; Clark, C. A.; Coonrod, C. L.; Wong, M. S. Treating water by degrading oxyanions using metallic nanostructures. *ACS Sustainable Chem. Eng.* **2018**, *6*, 11160−11175.

(3) Heck, K. N.; Garcia-Segura, S.; Westerhoff, P.; Wong, M. S. Catalytic converters for water treatment. *Acc. Chem. Res.* **2019**, *52*, 906−915.
(4) Chen, X.; Huo, X.; Liu, J.; Wang, Y.; Werth, C. J.; Strathmann, T. J. Exploring beyond palladium: Catalytic reduction of aqueous oxyanion pollutants with alternative platinum group metals and new mechanistic implications. *Chem. Eng. J.* **2017**, *313*, 745−752.
(5) Gao, J.; Ren, C.; Huo, X.; Ji, R.; Wen, X.; Guo, J.; Liu, J. Supported palladium catalysts: A facile preparation method and implications to reductive catalysis technology for water treatment. *ACS ES&T Engg* **2021**, *1*, 562−570.
(6) Ren, C.; Yang, P.; Gao, J.; Huo, X.; Min, X.; Bi, E. Y.; Liu, Y.; Wang, Y.; Zhu, M.; Liu, J. Catalytic reduction of aqueous chlorate with MoOx immobilized on Pd/C. *ACS Catal.* **2020**, *10*, 8201−8211.
(7) Ren, C.; Yang, P.; Sun, J.; Bi, E. Y.; Gao, J.; Palmer, J.; Zhu, M.; Wu, Y.; Liu, J. A bioinspired molybdenum catalyst for aqueous perchlorate reduction. *J. Am. Chem. Soc.* **2021**, *143*, 7891−7896.
(8) Liu, J.; Choe, J. K.; Sasnow, Z.; Werth, C. J.; Strathmann, T. J. Application of a Re−Pd bimetallic catalyst for treatment of perchlorate in waste ion-exchange regenerant brine. *Water Res.* **2013**, *47*, 91−101.
(9) Gu, B.; Brown, G. M.; Chiang, C.-C. Treatment of perchlorate-contaminated groundwater using highly selective, regenerable ion-exchange technologies. *Environ. Sci. Technol.* **2007**, *41*, 6277−6282.
(10) Ren, C.; Bi, E. Y.; Gao, J.; Liu, J. Molybdenum-catalyzed perchlorate reduction: Robustness, challenges, and solutions. *ACS ES&T Engg* **2022**, *2*, 181−188.
(11) Daimon, H.; Kurobe, Y. Size reduction of PtRu catalyst particle deposited on carbon support by addition of non-metallic elements. *Catal. Today* **2006**, *111*, 182−187.
(12) Weon, S.; Huang, D.; Rigby, K.; Chu, C.; Wu, X.; Kim, J.-H. Environmental materials beyond and below the nanoscale: Single-atom catalysts. *ACS ES&T Engg* **2021**, *1*, 157−172.
(13) Vorlop, K.-D.; Tacke, T. Erste schritte auf dem weg zur edelmetallkatalysierten nitrat-und nitrit-entfernung aus trinkwasser. *Chem. Ing. Tech.* **1989**, *61*, 836−837.
(14) Vorlop, K.-D.; Hörold, S.; Pohlandt, K. Optimierung von Trägerkatalysatoren zur selektiven Nitritentfernung aus Wasser. *Chem. Ing. Tech.* **1992**, *64*, 82−83.
(15) Prüsse, U.; Hörold, S.; Vorlop, K. D. Einfluß der präparationsbedingungen auf die eigenschaften von bimetallkatalysatoren zur nitratentfernung aus wasser. *Chem. Ing. Tech.* **1997**, *69*, 93−97.
(16) Hurley, K. D.; Shapley, J. R. Efficient heterogeneous catalytic reduction of perchlorate in water. *Environ. Sci. Technol.* **2007**, *41*, 2044−2049.
(17) Liu, J.; Choe, J. K.; Wang, Y.; Shapley, J. R.; Werth, C. J.; Strathmann, T. J. Bioinspired complex-nanoparticle hybrid catalyst system for aqueous perchlorate reduction: Rhenium speciation and its influence on catalyst activity. *ACS Catal.* **2015**, *5*, 511−522.
(18) Ren, C.; Liu, J. Bioinspired catalytic reduction of aqueous perchlorate by one single-metal site with high stability against oxidative deactivation. *ACS Catal.* **2021**, *11*, 6715−6725.
(19) Zhan, G.; Zeng, H. C. Charge-switchable integrated nano-catalysts for substrate-selective degradation in advanced oxidation processes. *Chem. Mater.* **2016**, *28*, 4572−4582.
(20) Wang, Y.; Liu, J.; Wang, P.; Werth, C. J.; Strathmann, T. J. Palladium nanoparticles encapsulated in core−shell silica: A structured hydrogenation catalyst with enhanced activity for reduction of oxyanion water pollutants. *ACS Catal.* **2014**, *4*, 3551−3559.
(21) Li, M.; Xu, F.; Li, H.; Wang, Y. Nitrogen-doped porous carbon materials: Promising catalysts or catalyst supports for heterogeneous hydrogenation and oxidation. *Catal. Sci. Technol.* **2016**, *6*, 3670−3693.
(22) Li, Z.; Yang, X.; Tsumori, N.; Liu, Z.; Himeda, Y.; Autrey, T.; Xu, Q. Tandem nitrogen functionalization of porous carbon: Toward immobilizing highly active palladium nanoclusters for dehydrogenation of formic acid. *ACS Catal.* **2017**, *7*, 2720−2724.
(23) Ye, T.; Banek, N. A.; Durkin, D. P.; Hu, M.; Wang, X.; Wagner, M. J.; Shuai, D. Pd nanoparticle catalysts supported on nitrogen-functionalized activated carbon for oxyanion hydrogenation and water purification. *ACS Appl. Nano Mater.* **2018**, *1*, 6580−6586.
(24) Zhang, Z.; Cheng, J.; Luo, Y.; Shi, W.; Wang, W.; Zhang, B.; Zhang, R.; Bao, X.; Guo, Y.; Cui, F. Pt nanoparticles supported on amino-functionalized SBA-15 for enhanced aqueous bromate catalytic reduction. *Catal. Commun.* **2018**, *105*, 11−15.
(25) Sun, J.; Zhang, J.; Fu, H.; Wan, H.; Wan, Y.; Qu, X.; Xu, Z.; Yin, D.; Zheng, S. Enhanced catalytic hydrogenation reduction of bromate on Pd catalyst supported on CeO_2 modified SBA-15 prepared by strong electrostatic adsorption. *Appl. Catal., B* **2018**, *229*, 32−40.
(26) Cai, L.; Hu, Z.; Branton, P.; Li, W. The effect of doping transition metal oxides on copper manganese oxides for the catalytic oxidation of CO. *Chin. J. Catal.* **2014**, *35*, 159−167.
(27) Cerrillo, J. L.; Lopes, C. W.; Rey, F.; Palomares, A. E. The influence of the support nature and the metal precursor in the activity of Pd-based catalysts for the bromate reduction reaction. *ChemCatChem* **2021**, *13*, 1230−1238.
(28) Chen, H.; Xu, Z.; Wan, H.; Zheng, J.; Yin, D.; Zheng, S. Aqueous bromate reduction by catalytic hydrogenation over Pd/Al_2O_3 catalysts. *Appl. Catal., B* **2010**, *96*, 307−313.
(29) Zhou, J.; Wu, K.; Wang, W.; Han, Y.; Xu, Z.; Wan, H.; Zheng, S.; Zhu, D. Simultaneous removal of monochloroacetic acid and bromate by liquid phase catalytic hydrogenation over Pd/$Ce_{1-x}Zr_xO_2$. *Appl. Catal., B* **2015**, *162*, 85−92.
(30) Zhang, Z.; Luo, Y.; Guo, Y.; Shi, W.; Wang, W.; Zhang, B.; Zhang, R.; Bao, X.; Wu, S.; Cui, F. Pd and Pt nanoparticles supported on the mesoporous silica molecular sieve SBA-15 with enhanced activity and stability in catalytic bromate reduction. *Chem. Eng. J.* **2018**, *344*, 114−123.
(31) Sun, W.; Li, Q.; Gao, S.; Shang, J. K. Highly efficient catalytic reduction of bromate in water over a quasi-monodisperse, superparamagnetic Pd/Fe_3O_4 catalyst. *J. Mater. Chem.* **2013**, *1*, 9215−9224.
(32) Li, M.; Zhou, X.; Sun, J.; Fu, H.; Qu, X.; Xu, Z.; Zheng, S. Highly effective bromate reduction by liquid phase catalytic hydrogenation over Pd catalysts supported on core-shell structured magnetites: Impact of shell properties. *Sci. Total Environ.* **2019**, *663*, 673−685.
(33) Zhang, P.; Jiang, F.; Chen, H. Enhanced catalytic hydrogenation of aqueous bromate over Pd/mesoporous carbon nitride. *Chem. Eng. J.* **2013**, *234*, 195−202.
(34) Biesinger, M.; Brown, C.; Mycroft, J.; Davidson, R.; McIntyre, N. X-ray photoelectron spectroscopy studies of chromium compounds. *Surf. Interface Anal.* **2004**, *36*, 1550−1563.
(35) Biesinger, M. C.; Payne, B. P.; Grosvenor, A. P.; Lau, L. W.; Gerson, A. R.; Smart, R. S. C. Resolving surface chemical states in XPS analysis of first row transition metals, oxides and hydroxides: Cr, Mn, Fe, Co and Ni. *Appl. Surf. Sci.* **2011**, *257*, 2717−2730.
(36) Veerakumar, P.; Lin, K.-C. An overview of palladium supported on carbon-based materials: Synthesis, characterization, and its catalytic activity for reduction of hexavalent chromium. *Chemosphere* **2020**, *253*, No. 126750.
(37) Oku, M.; Wagatsuma, K.; Konishi, T. Transition metal 2p x-ray photoelectron and high-resolution Kα x-ray emission spectra of K_2CrO_4 and $KMnO_4$. *X-Ray Spectrom.* **1999**, *28*, 464−469.
(38) Avena, M. J.; Giacomelli, C. E.; De Pauli, C. P. Formation of Cr(III) hydroxides from chrome alum solutions: 1. Precipitation of active chromium hydroxide. *J. Colloid Interface Sci.* **1996**, *180*, 428−435.
(39) Rai, D.; Sass, B. M.; Moore, D. A. Chromium (III) hydrolysis constants and solubility of chromium (III) hydroxide. *Inorg. Chem.* **1987**, *26*, 345−349.
(40) Thompson, M.; Connick, R. E. Hydrolytic polymerization of chromium(III). 1. Two dimeric species. *Inorg. Chem.* **1981**, *20*, 2279−2285.
(41) Stuenzi, H.; Marty, W. Early stages of the hydrolysis of chromium(III) in aqueous solution. 1. Characterization of a tetrameric species. *Inorg. Chem.* **1983**, *22*, 2145−2150.

https://doi.org/10.1021/acs.est.2c06468
Environ. Sci. Technol. 2023, 57, 1479−1486

(42) Sun, H.; Brocato, J.; Costa, M. Oral chromium exposure and toxicity. *Curr. Environ. Health Rep.* **2015**, *2*, 295−303.
(43) Sun, W.; Li, Q.; Gao, S.; Shang, J. K. Monometallic Pd/Fe_3O_4 catalyst for denitrification of water. *Appl. Catal., B* **2012**, *125*, 1−9.
(44) Feng, X.; Zhang, B.; Chery, L. Effects of low temperature on aluminum(III) hydrolysis: Theoretical and experimental studies. *J. Environ. Sci.* **2008**, *20*, 907−914.
(45) Papassiopi, N.; Vaxevanidou, K.; Christou, C.; Karagianni, E.; Antipas, G. Synthesis, characterization and stability of Cr(III) and Fe(III) hydroxides. *J. Hazard. Mater.* **2014**, *264*, 490−497.

https://doi.org/10.1021/acs.est.2c06468
Environ. Sci. Technol. 2023, 57, 1479−1486